



Zarif Karimi, N., Heidary, H., Minak, G., & Fotouhi, M. (2017).  
Experimental analysis of GFRP laminates subjected to compression  
after drilling. *Composite Structures*, 169, 144–152.  
<https://doi.org/10.1016/j.compstruct.2017.01.017>

Peer reviewed version

License (if available):  
CC BY-NC-ND

Link to published version (if available):  
[10.1016/j.compstruct.2017.01.017](https://doi.org/10.1016/j.compstruct.2017.01.017)

[Link to publication record in Explore Bristol Research](#)  
PDF-document

This is the author accepted manuscript (AAM). The final published version (version of record) is available online via Elsevier at <http://www.sciencedirect.com/science/article/pii/S0263822316314003>. Please refer to any applicable terms of use of the publisher.

## University of Bristol - Explore Bristol Research

### General rights

This document is made available in accordance with publisher policies. Please cite only the published version using the reference above. Full terms of use are available:  
<http://www.bristol.ac.uk/red/research-policy/pure/user-guides/ebr-terms/>

# Experimental analysis of GFRP laminates subjected to compression after drilling

Navid Zarif Karimi <sup>1\*</sup>, Hossein Heidary<sup>2</sup>, Mohamad Fotouhi <sup>3</sup>, Giangiacomo Minak <sup>2</sup>

1- University of Bologna, Department of Industrial Engineering DIN, Viale del Risorgimento 2, 40136, Bologna, Italy, [navid.zarif@unibo.it](mailto:navid.zarif@unibo.it), [giangiacomo.minak@unibo.it](mailto:giangiacomo.minak@unibo.it)

2- University of Tafresh, Department of Mechanical Engineering, First of Tehran Road, 7961139518 Tafresh, Iran  
[heidary@tafreshu.ac.ir](mailto:heidary@tafreshu.ac.ir)

3- Advanced Composites Centre for Innovation and Science, University of Bristol, Bristol BS8 1TR, UK  
[m.fotouhi@bristol.ac.uk](mailto:m.fotouhi@bristol.ac.uk)

## ABSTRACT

Drilling is one of the most frequently used machining processes for glass fiber reinforced polymer composites due to the need for structural joining. In the drilling of composite laminates, Interlaminar cracking, or delamination has a detrimental effect on compressive strength of these materials. The delamination can be controlled by adopting proper drilling conditions. In this paper, the effects of feed rate and cutting speed on delamination and residual compressive strength of drilled GFRPs are studied. The objective is to find the optimal conditions for maximum residual compressive strength.

**Keywords:** Composite materials, Delamination, Drilling, Residual compressive strength.

## 1. Introduction

Glass fiber reinforced plastics (GFRPs) are characterized by having a combination of high specific strength, high stiffness, and weight saving. As a result of these remarkable properties, GFRPs have attracted increasing attention for use in many industries [1]. However, GFRPs have specific characteristics that affect their machining behavior. The mechanisms of cutting composite materials are considerably distinct from those observed during cutting isotropic materials. Application expansion of composite materials calls for the use of different types of machining among them conventional drilling with twist drill is one of the most commonly used processes in the assembly of composite sub-components. However, some damages occur during drilling such as delamination, fiber pull out, matrix burning, etc. which degrade mechanical properties of the composite structures [2, 3].

One of the most common damage mechanisms in GFRPs is **the(?)** delamination, in which the layers of the material separate from each other. Delamination can be caused due to localized bending in the zone sited at the point of drill contact. The interface is weaker in transverse

strength as compared to the layers. Hence, its failure is dominated by the transverse stresses. The interface generally fails under tensile load applied normal to it. In addition, the delamination can take place due to compressive stresses in its in-plane direction causing buckling, which in turn, causes delamination. Delamination reduces the strength and stiffness and thus limits the life of a structure. Further, it causes stress concentration in load bearing plies and a local instability leading to a further growth of delamination that results in a compressive failure of the laminate. In these two cases, delamination leads to a redistribution of structural load paths that, in turn, precipitates structural failure. Hence, delamination indirectly affects the final failure of the structure thus affecting its life. Therefore, delamination is known as the most prevalent life-limiting damage growth mode [4, 5].

Depending on the size of the delamination, it can reduce the static and fatigue strength and the compression buckling strength. In order to measure the amount of delamination quantitatively, Chen [6] proposed an approach to obtain the value of the conventional delamination factor which assumes the form as Eq. (1). The conventional delamination factor is not appropriate owing to the fact that the crack size does not represent the damage magnitude properly. Furthermore, this procedure does not indicate the damage area. A novel approach devised to measure the delamination factor was proposed by Davim et al. [7], namely the adjusted delamination factor, and calculated through Eq. (2). The first part of Eq. (2) shows the size of the crack contribution and the second part shows the damage area contribution.

$$F_d = \frac{D_{\max}}{D_0} \quad (1)$$

$$F_{da} = \alpha \frac{D_{\max}}{D_0} + \beta \frac{A_{\max}}{A_0} \quad (2)$$

The coefficients  $\alpha$  and  $\beta$  are calculated as below;

$$\beta = \frac{A_d}{A_0 - A_{\max}} \quad \text{and} \quad \alpha = 1 - \beta \quad (3)$$

where  $D_0$  is the nominal diameter of the hole,  $D_{\max}$  is the maximum diameter of the damage hole,  $A_0$  is the area related to the nominal hole,  $A_{\max}$  is the area related to the maximum diameter of the delamination zone and  $A_d$  is the delaminated area. Different parameters used in preceding equations are illustrated in Fig. 1.

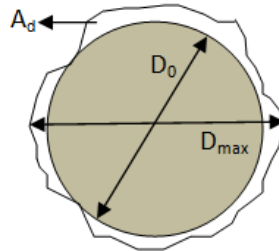


**Figure 1.** Measurement of delamination factor.

In order to reduce the delamination, it is necessary to develop procedures to select appropriate cutting parameters, because an unsuitable choice could lead to unacceptable work material degradation. Several researchers investigated the effects of input variables, feed rate, cutting speed, and point angle of twist drill bit, on drilling-induced delamination. Davim and Reis et al. [8-11] conducted a series of experiments on different composite materials including GFRPs, CFRPs, and metal matrix composites to understand the effects of drilling parameters on delamination and other characteristics of these materials. Their results show that delamination increases with feed rate and cutting speed. The effect of feed rate on delamination is more than that of cutting speed. Unlike them, the works conducted by Khashaba [12, 13] show that delamination decreases with cutting speed during drilling of woven-ply GFRP composite laminates; Gaitonde et al. [14] also reported that delamination decreases with cutting speed during high speed drilling of thin woven-ply CFRP composite laminates. They also observed that delamination increased by increasing drill point angle of drill bit. However, Kilickap [15] observed that the delamination tendency decreased with increase of point angle of twist drill during conventional drilling of UD-ply GFRP composite laminates. To summarize, almost all researchers reported that drilling-induced delamination increased with feed rate at any different cutting speed using various drill bits, while two different behavior for cutting speed and drill point angle were observed.

A few researchers studied the effect of cutting parameters on mechanical properties of drilled composites. Persson et al. [16] investigated the effect of hole machining damages on strength and fatigue life of carbon/epoxy laminates subjected to static and fatigue loads. They observed that hole machining damages significantly reduced the static and fatigue strengths of pin-loaded laminates; the effects on the strengths of compressively loaded laminates were less pronounced. Kishore et al. [17] studied the effect of the cutting speed, the feed rate, and the drill point geometry on the residual tensile strength of the drilled unidirectional glass fiber reinforced epoxy composites. They observed that feed rate had least influence and the cutting speed had maximum influence on residual tensile strength, and it increased substantially with an increase in cutting speed. Unlike them, Zarif et al. [18] observed that feed rate had the most important effect and cutting speed had the least effect on residual tensile strength of drilled woven glass/epoxy composites. Tagliaferri et al. [19] studied the tensile strength of the drilled specimens of GFRPs and found it to be independent of the damage extent. The bearing strength was, however, influenced by the damage and a reduction in damage was accompanied by an increase in the bearing strength. Capello and Tagliaferri [20, 21] investigated the influence of the drilling conditions on the residual mechanical behavior of the glass fiber reinforced composites subjected to a bearing load. They found that in order to improve the static bearing load (SBL) behavior of drilled holes, lower feed rate should be employed with the use of backing plate.

Although much researched have been done to understand the effects of drilling parameters on delamination and tensile strength of drilled laminates, none to date has studied the effect cutting

parameters on residual compressive strength of composite laminates. This paper aims to study the effect of cutting parameters, feed rate and spindle speed, on the residual compressive strength of drilled GFRPs.

## 2. Experimental procedure

### 2.1. Materials and methods

The composite specimens for drilling tests were manufactured by hand lay-up method from Araldite LY556 epoxy resin reinforced with high strength E-glass woven fiber. The GFRP laminates were approximately 6 mm thick consisting of 12 plies and had an approximately 50% fiber volume fraction. After preparation, specimens of size 100 mm  $\times$  150 mm were cut according to the ASTM Standard D7137 / D7137M [22].

All drilling experiments were conducted on the ANILAM radial drilling machine. To fix the specimens in the drilling machine an appropriate clamping system was used, shown in Fig. 2(a). The standard HSS twist drills of 5 mm diameter were used for the experimental program. The tool was changed after every 5 experiments to avoid tool wear, and all tests were run without coolant. The holes were generated at the center of the specimen and each experiment was replicated three times. The compression experiments were carried out on an Instron 8033 testing machine.

The instrumentation and loading arrangement of the specimens in the buckling test rig is shown in Fig. 2(b). All sides of the specimen are completely supported; the two vertical edges are supported in knife edges and the two horizontal edges supported in fixed supports. All specimens were loaded at a constant speed of 1.5 mm/min until failure.



**Figure 2.** Experimental setup (a) drilling, (b) compression.

### 2.2. Plan of experiments

Drilling experiments were designed based on general full factorial design. Full factorial design means that in each complete trial or replication of the experiment all possible combinations of the levels of the factors are investigated. In some experiments, the difference in response

between the levels of one factor is not the same at all levels of the other factors. When this occurs, there is an interaction between the factors. A factorial design is necessary when interactions may be present to avoid misleading conclusions. Furthermore, factorial designs allow the effects of a factor to be estimated at several levels of the other factors, yielding conclusions that are valid over a range of experimental conditions. Minitab16 was used to create the design matrix and analyze the results as statistical software. Two factors i.e. feed rate and spindle speed at three levels were used as input factors and delamination factor and residual compressive strength were considered as the main response factors. Input factors and their corresponding levels are given in Table 1.

### 3. Results

After conducting drilling tests, the drilled holes were scanned with a digital scanner. Then, the scanned images were imported to a CAD software to determine the delamination factor according to Eq. (1).

Afterward, all drilled specimens were compression tested to find ultimate compression force. The values of residual compressive strength were calculated as the ratio of ultimate force to the remained section area after drilling, expressed as below:

$$\sigma_r = \frac{F_U}{(w-d)t} \quad (4)$$

where  $F_u$ ,  $d$ ,  $w$  and  $t$  are the ultimate compression force, the hole diameter, the specimen width and specimen thickness, respectively.

The design matrix, measured delamination factor, and residual compressive strength are reported in Table 1.

**Table 1.** The design matrix and measured experimental results.

Test No.	Parameters		$F_{da}$			$\sigma_r$ (MPa)		
	Feed rate (mm/min)	Spindle speed (rpm)	R1	R2	R3	R1	R2	R3
1	31.5	315	1.09	1.10	1.08	433.3	412.3	408.8
2	31.5	630	1.10	1.07	1.08	366.7	373.7	371.9
3	31.5	1000	1.07	1.04	1.05	450.9	426.3	417.5
4	63	315	1.12	1.13	1.11	359.6	363.2	352.6
5	63	630	1.15	1.15	1.12	338.6	331.6	329.8
6	63	1000	1.10	1.11	1.15	370.2	377.2	387.7
7	125	315	1.18	1.19	1.17	312.3	308.8	312.3
8	125	630	1.15	1.16	1.13	315.8	331.6	321.1
9	125	1000	1.13	1.08	1.11	305.3	298.2	305.3

The analysis of variance for delamination is shown in Table 2. Because  $F_{0.05,4,18}=2.93$ , it can be concluded that there is a significant interaction between feed rate and spindle speed. Moreover,  $F_{0.05,2,18}=3.55$ , so the main effects of feed rate and spindle speed are also significant. Table 2. also shows the  $P$ -value for the test statistics. The adequacy of the model and further analysis were done in authors' previous paper [23].

**Table 2.** Analysis of variance for delamination.

Source of Variation	Sum of Squares	Degrees of Freedom	Mean Square	$F_0$	P-Value	Contribution Percentage (%)
Feed rate	0.0230222	2	0.0115111	39.34	0.0001	56.8
Speed	0.0068667	2	0.0034333	11.73	0.001	15.9
Interaction	0.0043111	4	0.0010778	3.68	0.023	7.9
Error	0.0052667	18	0.0002926			19.4
Total	0.0394667	26				

The analysis of variance for residual compressive strength is summarized in Table 3. According to the  $P$ -value column, we see that the feed rate and spindle speed significantly affect the residual compressive strength. The feed rate-spindle speed interaction has  $P$ -value of  $<0.0001$ , indicating significant interaction between these factors. To assist in the practical interpretation of the experiment, Fig. 3 presents plots of the two main effects. The main effect plots are just graphs of the response averages at the levels of the two factors. Notice that the feed rate has negative effect; that is, increasing the feed rate moves the average response downward. While, the spindle speed has a negative effect at the beginning and then its effect changes to positive. Table 3. also shows contribution percentage of the factors and their interaction. The feed rate has the most contribution percentage, indicating it has the greatest effect on residual compressive strength.

**Table 3.** Analysis of variance for residual compressive strength.

Source of Variation	Sum of Squares	Degrees of Freedom	Mean Square	$F_0$	P-Value	Contribution Percentage (%)
Feed rate	40253	2	20126.7	257.93	0.0001	77.9
Spindle Speed	3904	2	1952.1	25.02	0.0001	7.3
Interaction	5872	4	1468.1	18.81	0.0001	10.7
Error	1405	18	78.0			4.1
Total	51434	26				

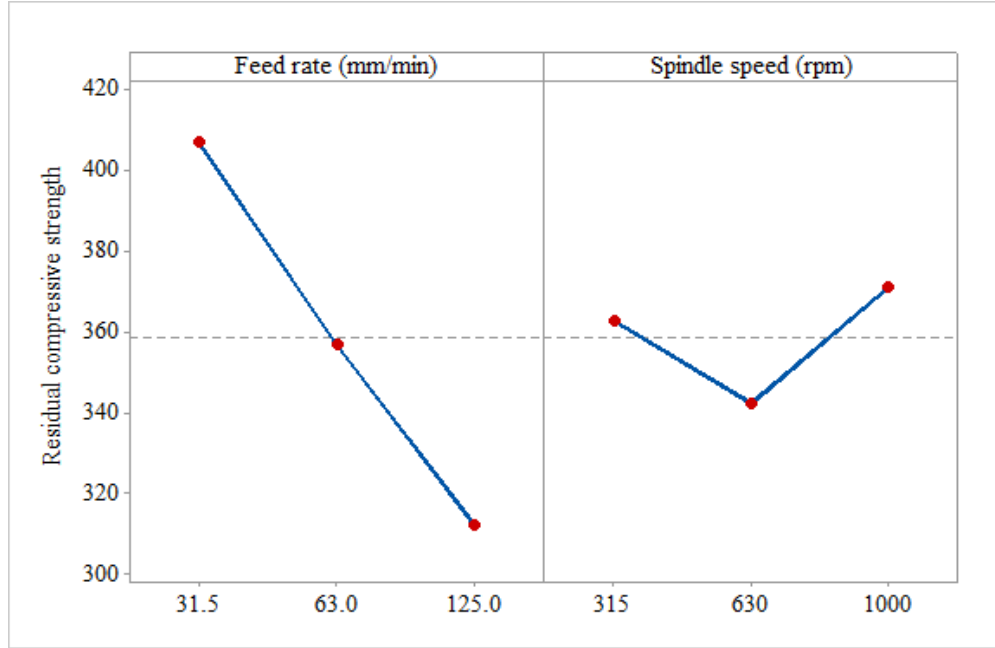


**Figure 3.** Main effects plot for compressive strength.

One of the main feature of analysis of variance is the adequacy of the underlying model. For this purpose, residual analysis is used as primary diagnostic tool. Through a study of residuals, many types of model adequacies and violations of the underlying assumptions can be discovered. The residuals for two-factor factorial model are:

$$e_{ijk} = y_{ijk} - \hat{y}_{ijk} \quad (5)$$

where  $y_{ijk}$  is the observed response when feed rate is at the  $i$ -th level and spindle speed is at the  $j$ -th level for the  $k$ -th replicate.

The residuals from the compressive strength data are shown in the Fig. 4. A check of normality assumption could be made by plotting a histogram of the residuals, Fig .4(a). Notice that this plot looks look a normal distribution centered at zero, indicating the normality assumption is satisfied. Also, the normal probability plot, Fig. 4(b), shows nothing particularly troublesome. If the model is adequate, the residuals should be structureless; that is, they should contain no obvious patterns. A simple check is to plot the residuals versus the fitted values. From Fig. 4(c) no unusual structure is apparent. Plotting residuals in time order of data collection is helpful in detecting correlation between the residuals. A plot of these residuals versus time is shown in Fig. 4(d). There is no reason to suspect any violation of the independence or constant variance assumptions.

Fig. 5(a) and Fig. 5(b) plot the residual versus feed rate and spindle speed, respectively. Both plots indicate mild inequality of variance. Two treatments, (31.5 mm/min and 315 rpm) and (31.5 mm/min and 1000 rpm), have larger variance than the others, which are responsible for the



inequality of the variance. These are the only two positive residuals whose absolute values are greater than 2. However, this problem is not severe enough to have a dramatic impact on the analysis and conclusions.

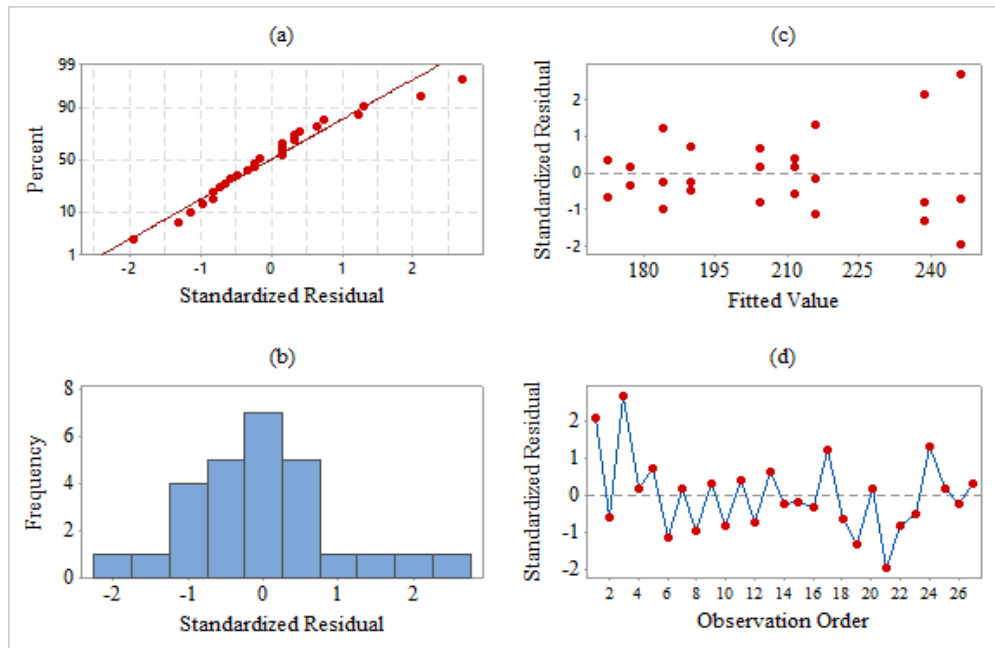


**Figure 4.** Residual plots for compressive strength.

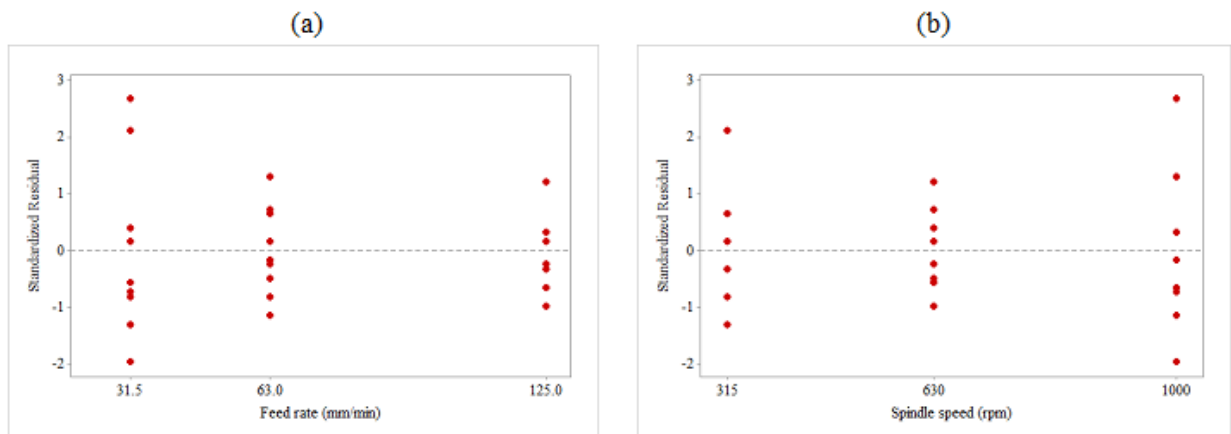


**Figure 5.** Plot of standardized residuals versus (a) feed rate, (b) spindle speed.

To understand the interaction between factors, the graph of the average responses at each treatment combination is shown in Fig. 6(a). The significant interaction is indicated by the lack of parallelism of the lines when feed rate is kept high. Notice that at low and medium levels of feed rate, the interaction is fairly small, as shown by the similar shape of the two curves. Fig. 6(b) presents a contour plot of the surface generated by the prediction model for residual compressive strength. The contour plot indicates that the feed rate of 31.5 mm/min and spindle speed of 1000 rpm are the best choices to achieve maximum compression strength.

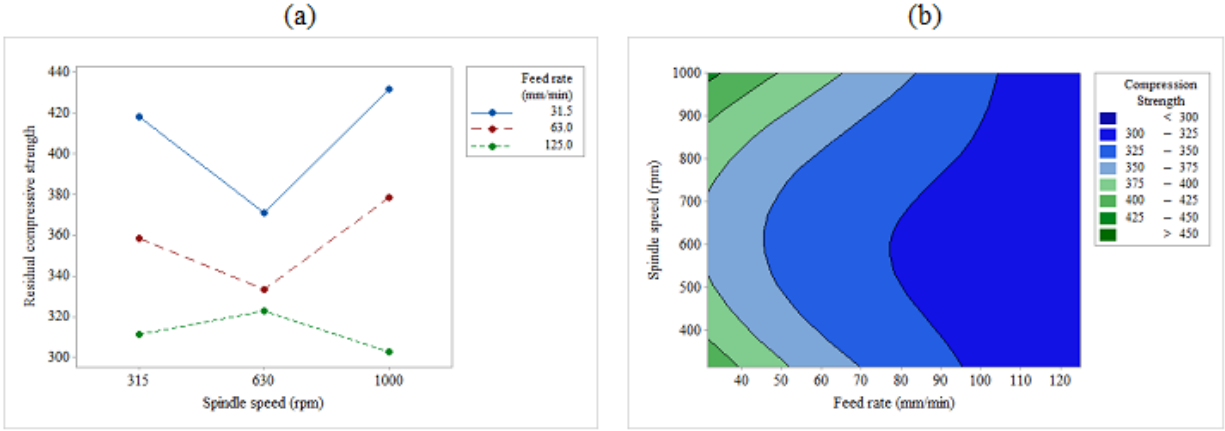


**Figure 6.** The interaction plot and, (b) the counter plot of compressive strength.

To make a mathematical model showing the relationship between feed rate and spindle speed as input factors and residual compressive strength as response, polynomial regression model was adopted. Matlab software was used to generate the regression model and the result is shown in Eq. (6). This equation is useful for interpolation, that is, for predicting the residual compressive strength ( $\sigma_r$ ) at factor levels between those actually used in the experiment. Fig. (7) shows response surface of corresponding regression model.

$$\sigma_r = 519.8 - 2.188f - 0.2276N + 0.009347f^2 - 0.0004411fN + 0.0002069N^2$$

$$R^2 = 0.8706 \quad R_{adj}^2 = 0.8398$$

(6)

being,  $f$  the feed rate in mm/min and  $N$  the cutting speed in rpm.

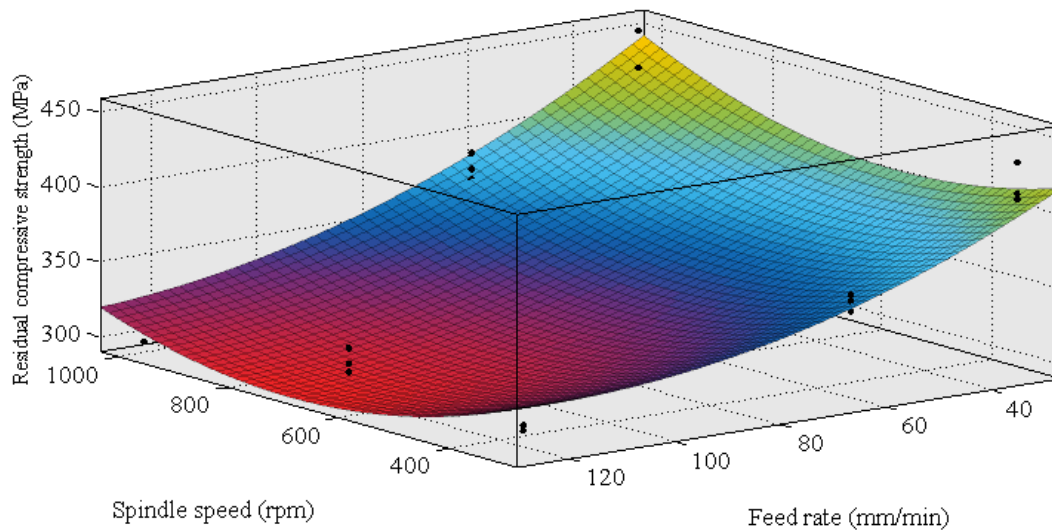


**Figure 7.** The response surface of polynomial regression model for residual compressive strength.

#### 4. Conclusion

In the current paper, the effect of drilling parameters on delamination and residual compressive strength of drilled GFRPs was investigated experimentally. Two drilling parameters i.e. feed rate and spindle speed at three levels, based on the full factorial design, were studied. Optimum drilling conditions for maximum residual strength was determined based on analysis of variance. The effect of feed rate on residual compressive strength was much more than that of cutting speed. Also, the relationship between feed rate, spindle speed and residual compressive strength was presented by polynomial regression model.

#### References

1. Chung, D.D.L., *Composite Materials: Science and Applications*. 2010: Springer London.
2. Liu, D., Y. Tang, and W.L. Cong, *A review of mechanical drilling for composite laminates*. *Composite Structures*, 2012. **94**(4): p. 1265-1279.
3. Hocheng, H., *Machining technology for composite materials: principles and practice*. 2011: Elsevier.
4. Gibson, R.F., *Principles of composite material mechanics*. 2011: CRC Press.
5. Krishnaraj, V., R. Zitoun, and J.P. Davim, *Drilling of polymer-matrix composites*. 2013: Springer.
6. Chen, W.-C., *Some experimental investigations in the drilling of carbon fiber-reinforced plastic (CFRP) composite laminates*. *International Journal of Machine Tools and Manufacture*, 1997. **37**(8): p. 1097-1108.
7. Davim, J.P., J.C. Rubio, and A.M. Abrao, *A novel approach based on digital image analysis to evaluate the delamination factor after drilling composite laminates*. *Composites Science and Technology*, 2007. **67**(9): p. 1939-1945.
8. Basavarajappa, S., G. Chandramohan, and J.P. Davim, *Some studies on drilling of hybrid metal matrix composites based on Taguchi techniques*. *Journal of Materials Processing Technology*, 2008. **196**(1-3): p. 332-338.

9. Krishnamoorthy, A., et al., *Application of grey fuzzy logic for the optimization of drilling parameters for CFRP composites with multiple performance characteristics*. Measurement, 2012. **45**(5): p. 1286-1296.
10. Grilo, T.J., et al., *Experimental delamination analyses of CFRPs using different drill geometries*. Composites Part B: Engineering, 2013. **45**(1): p. 1344-1350.
11. Pinho, L., D. Carou, and J. Davim, *Comparative study of the performance of diamond-coated drills on the delamination in drilling of carbon fiber reinforced plastics: assessing the influence of the temperature of the drill*. Journal of Composite Materials, 2016. **50**(2): p. 179-189.
12. Khashaba, U.A., *Delamination in drilling GFR-thermoset composites*. Composite Structures, 2004. **63**(3-4): p. 313-327.
13. Khashaba, U.A., et al., *Machinability analysis in drilling woven GFR/epoxy composites: Part I – Effect of machining parameters*. Composites Part A: Applied Science and Manufacturing, 2010. **41**(3): p. 391-400.
14. Gaitonde, V.N., et al., *Analysis of parametric influence on delamination in high-speed drilling of carbon fiber reinforced plastic composites*. Journal of Materials Processing Technology, 2008. **203**(1-3): p. 431-438.
15. Kilickap, E., *Optimization of cutting parameters on delamination based on Taguchi method during drilling of GFRP composite*. Expert Systems with Applications, 2010. **37**(8): p. 6116-6122.
16. Persson, E., I. Eriksson, and L. Zackrisson, *Effects of hole machining defects on strength and fatigue life of composite laminates*. Composites Part A: Applied Science and Manufacturing, 1997. **28**(2): p. 141-151.
17. Kishore, R.A., et al., *Taguchi analysis of the residual tensile strength after drilling in glass fiber reinforced epoxy composites*. Materials & Design, 2009. **30**(6): p. 2186-2190.
18. Zarif Karimi, N., H. Heidary, and M. Ahmadi, *Residual tensile strength monitoring of drilled composite materials by acoustic emission*. Materials & Design, 2012. **40**(0): p. 229-236.
19. Tagliaferri, V., G. Caprino, and A. Diterlizzi, *Effect of drilling parameters on the finish and mechanical properties of GFRP composites*. International Journal of Machine Tools and Manufacture, 1990. **30**(1): p. 77-84.
20. Capello, E. and V. Tagliaferri, *Drilling damage of GFRP and residual mechanical behavior-part I: drilling damage generation*. Journal of composites technology & research, 2001. **23**(2): p. 122-130.
21. Capello, E. and V. Tagliaferri, *Drilling damage of GFRP and residual mechanical behavior-part II: static and cyclic bearing loads*. Journal of composites technology & research, 2001. **23**(2): p. 131-137.
22. *ASTM D7137 / D7137M-12, Standard Test Method for Compressive Residual Strength Properties of Damaged Polymer Matrix Composite Plates*, ASTM International, West Conshohocken, PA, 2012,.
23. Zarif Karimi, N., G. Minak, and P. Kianfar, *Analysis of damage mechanisms in drilling of composite materials by acoustic emission*. Composite Structures, 2015. **131**(0): p. 107-114.

### **Figure Caption:**

**Figure 1.** Measurement of delamination factor.

**Figure 2.** Experimental setup (a) drilling, (b) compression.

**Figure 3.** Main effects plot for compressive strength.

**Figure 4.** Residual plots for compressive strength.

**Figure 5.** Plot of standardized residuals versus (a) feed rate, (b) spindle speed.

**Figure 6.** The interaction plot and, (b) the counter plot of compressive strength.

**Figure 7.** The response surface of polynomial regression model for residual compressive strength.

### **Table Caption:**

**Table 1.** The design matrix and measured experimental results.

**Table 2.** Analysis of variance for delamination.

**Table 3.** Analysis of variance for residual compressive strength.